Am J Cancer Res 2026;16(2):639-649
www.ajcr.us /ISSN:2156-6976/ajcr0169719

Original Article

PDE4C stabilized by ELAVL1 promotes lymph node metastasis in papillary thyroid cancer

Tingting Cui[1,2], Ying Zhang[2], Wanwan Li[3], Danzhen Zhang[2], Weida Liu[1], Haiying Gong[4]

[1]*Department of Ultrasound, Taizhou Traditional Chinese Medicine Hospital, Jiaojiang 318000, Zhejiang, China;* [2]*Department of Medical, Taizhou Traditional Chinese Medicine Hospital, Jiaojiang 318000, Zhejiang, China;* [3]*Department of Otolaryngology, Taizhou Traditional Chinese Medicine Hospital, Jiaojiang 318000, Zhejiang, China;* [4]*Department of Ultrasound, Yiwu Traditional Chinese Medicine Hospital, Yiwu 322000, Zhejiang, China*

Received November 1, 2025; Accepted February 24, 2026; Epub February 25, 2026; Published February 28, 2026

Abstract: Lymph node metastasis (LNM) is a key factor in the recurrence and progression of papillary thyroid carcinoma (PTC). Phosphodiesterase 4C (PDE4C) serves as a crucial regulator in cancer development and metastasis, its functional role and mechanism in LNM of PTC need further elucidation. PDE4C and embryonic lethal abnormal vision like 1 (ELAVL1) expression in PTC and adjacent normal tissues were assessed using bioinformatic analysis and immunohistochemistry (IHC). We found that PDE4C and ELAVL1 were upregulated in PTC tissues. Cell viability in BCPAP and TPC-1 cell lines was assessed via cell counting kit-8 (CCK-8) assay, while Transwell assays were employed to determine their migratory and invasive capacities. Our data revealed that silencing of PDE4C remarkably suppressed BCPAP and TPC-1 cell proliferation, migration and invasion. Besides, the association between ELAVL1 and PDE4C was predicted and verified by ENCORI, RNA pull down and RNA immunoprecipitation (RIP) assay. The mRNA of ELAVL1 and PDE4C were evaluated via quantitative real-time PCR (qRT-PCR). ELAVL1 and PDE4C expression was examined using Western blot analysis. The number of metastatic tumors in the lymph nodes was assessed by hematoxylin-eosin (HE) staining. Ki-67 level in tumor tissues were determined by IHC. ELAVL1 interacts with PDE4C, resulting in an increase in PDE4C mRNA stability, which contributes to the aforementioned malignant phenotypes. Consistently, the knockdown of PDE4C or ELAVL1 inhibited LNM of PTC cells, PTC growth, and Ki-67 expression *in vivo*. In summary, ELAVL1 promotes LNM in PTC by stabilising PDE4C. Our study elucidates the molecular mechanisms driving PTC metastasis, offering new therapeutic avenues for PTC treatment.

Keywords: Phosphodiesterase 4C (PDE4C), embryonic lethal abnormal vision like 1 (ELAVL1), lymph node metastasis, papillary thyroid cancer

Introduction

Thyroid cancer is the most prevalent endocrine malignancy, with a persistently rising global incidence rate [1]. Papillary thyroid carcinoma (PTC), accounting for approximately 85% of all thyroid cancer cases, represents the predominant histological subtype [2]. Although multimodal approaches combining surgery with radioactive iodine therapy have yielded favourable outcomes for most patients with PTC [3, 4], approximately 40% of adult patients develop lymph node metastases (LNM) [5]. Some cases even exhibit extrathyroidal invasion or distant organ metastases, substantially increasing the risk of tumor recurrence [6, 7]. Therefore, elucidating the molecular mechanisms underlying PTC metastasis is crucial for achieving early diagnosis of lymph node spread and developing novel targeted therapies.

The phosphodiesterase (PDE) family serves as a key regulatory enzyme in the cAMP signaling pathway, critically influencing cellular functions including proliferation and migration [8]. Phosphodiesterase 4C (PDE4C), a member of the PDE family, has been increasingly recognized for its involvement in oncogenesis [9]. Researches have shown that PDE4C is significantly upregulated in thyroid cancer, suggesting its potential as a poor prognostic marker [10]. In addition, M2 macrophage-derived PDE4C facilitates osteosarcoma progression by enhancing collagen-mediated proliferation and

https://doi.org/10.62347/VZMV3943

migration [11]. A study by Pan et al. suggested that PDE4C promotes osteosarcoma cell proliferation and migratory capacity through upregulation of intracellular collagen expression [11]. It is worth noting that the function of PDE4C in thyroid cancer and other tumors has been partially supported by experimental evidence; however, the specific molecular mechanism of PDE4C in PTC remain to be fully elucidated.

Embryonic lethal abnormal vision like 1 (ELAVL1), an essential RNA-binding protein, plays a pivotal role in regulating fundamental cellular processes, including proliferation, stress, and apoptosis [12]. ELAVL1 has been demonstrated to facilitate tumor progression and metastasis in malignancies through enhancing the stability of downstream target mRNAs, including gastric cancer [13], breast cancer, and prostate cancer [14, 15]. In addition, ELAVL1 was evidenced to be involved in the regulation of proliferation, migration, and invasion of PTC cells [16]. ENCORI database prediction revealed the potential binding interaction between ELAVL1 and PDE4C mRNA. Nevertheless, the role and detailed mechanism of ELAVL1 in LNM of PTC still need to be explored.

Thus, we propose that ELAVL1 upregulates PDE4C expression by stabilizing its mRNA, thereby facilitating LNM in PTC. Our study elucidates the functional roles of PDE4C and ELAVL1 in PTC cell lines, and in vivo tumor metastasis models, providing new perspectives for the diagnosis and treatment of PTC.

Materials and methods

Clinical specimens

A total of 20 untreated PTC patients undergoing surgery at Taizhou Traditional Chinese Medicine Hospital provided matched tumor and paratumoral tissue samples. These specimens were rapidly frozen and stored at -80°C until further analysis. The research project was sanctioned by the Institutional Ethics Committee (Taizhou Traditional Chinese Medicine Hospital Ethics Committee; Protocol No.: LL2025-LW-023), and all participants provided written informed consent prior to participation.

Bioinformatics database

To explore the expression pattern of PDE4C in thyroid carcinoma, we employed two independent bioinformatics platforms. GEPIA2 (http://gepia2.cancer-pku.cn/) was employed to examine the differential expression of PDE4C and ELAVL1 between malignant and non-malignant thyroid tissues. Furthermore, PDE4C and ELAVL1 expression in tumor tissues and corresponding normal tissues was evaluated through the UALCAN database (http://ualcan.path.uab.edu/index.html). ENCORI (http://starbase.sysu.edu.cn/) was conducted to assess the binding potential of ELAVL1 to PDE4C mRNA.

Cell culture

Human PTC cell lines BCPAP (RRID: CVCL_0153; SCSP-543, Chinese Academy of Sciences, Shanghai, China) and TPC-1 (RRID: CVCL_6298; JNO-H0390, Guangzhou Jennio Biotech Co., Ltd., China), both derived from the thyroid glands of female PTC patients, were maintained in RPMI-1640 medium (11875093, Invitrogen) containing 10% fetal bovine serum (FBS; C9500, New Cell & Molecular Biotech Co., Ltd., Suzhou, China), 1% streptomycin/penicillin (C0222, Beyotime, Shanghai, China) at 37°C under 5% CO_2. All cell lines underwent STR authentication and were confirmed to be free of mycoplasma contamination.

Cell transfection

The overexpression plasmid pcDNA3.1-PDE4C (oe-PDE4C), shRNA sequences targeting ELAVL1 (sh-ELAVL1-1/2) or PDE4C (sh-PDE4C-1/2), and their respective negative control vectors (oe-NC and sh-NC) were provided by Genechem (Shanghai, China). Lipofectamine 3000 (Invitrogen) was employed for cell transfection. To achieve PDE4C overexpression, the coding sequence was PCR-amplified from PDE4C cDNA and then cloned into the pcDNA3.1 vector at the BamHI/EcoRI restriction sites. For gene silencing experiments, shRNA sequences designed to target ELAVL1 or PDE4C were inserted into pLKO.1 vector.

Cell Counting Kit-8 (CCK-8) assay

Cell Counting Kit-8 (C6050, New Cell & Molecular Biotech) was utilized to test the cells proliferation ability. PTC cell lines (4000 cells/well) were plated in 96-well plates. After treatment, 10 μL of the CCK-8 solution was added to the wells, and incubated for 2 h. Next, the

Table 1. Primer sequences used in this study

Gene	Forward primer	Reverse primer
ELAVL1	5'-TGTTCTCTCGGTTTGGGCGGAT-3'	5'-TCTTCTGCCTCCGACCGTTTGT-3'
PDE4C	5'-AGGTCACTACCACGCCAATGTG-3'	5'-CAGCCAGGATTTCCAAGTCTGTG-3'
β-actin	5'-CACCATTGGCAATGAGCGGTTC-3'	5'-AGGTCTTTGCGGATGTCCACGT-3'

$OD_{450\ nm}$ was assessed on a microplate reader (BMG LABTECH, Germany).

Cell migration and invasion assays

Cell migratory and invasive capacities were assessed using Transwell chambers (CLS3428, Corning). For invasion assay, the Transwell membranes were pre-coated with Matrigel (Corning), diluted in serum-free medium, and cultivated overnight at 37°C. In both migration and invasion assays, we seeded 2×10^5 cells into the upper chamber and suspended cells in 200 μL of serum-free medium. Moreover, the lower chamber was added with 600 μL of complete medium containing 10% FBS. After 24-48 h incubation, the migrated or invaded cells to the lower surface were fixed with 4% paraformaldehyde for 30 min, stained with 0.1% crystal violet for 20 min, and visualized under an inverted microscope (Zeiss, Germany).

RNA pull-down assay

The connection between PDE4C mRNA and ELAVL1 was confirmed via the The Pierce™ Magnetic RNA-Protein Pull-Down Kit (20164, Thermo Scientific). In short, cells were subjected to lysis using Lysis Buffer, and the lysates were centrifuged at 13,000×g for 10 min at 4°C, and the resulting supernatant was obtained. Next, the supernatant was incubated with a biotin-labeled PDE4C RNA probe for 4 h to form RNA-protein complex. The mixture was subjected to magnetic bead capture using Streptavidin Magnetic Beads to isolate the RNA-bound protein complexes. After 3 washes with wash buffer, the captured proteins were eluted using an elution buffer. Finally, Western blotting was performed to detect ELAVL1 level.

RNA immunoprecipitation (RIP)

Magna RIP Immunoprecipitation Kit (17-700, Millipore) was applied for evaluating the interaction between ELAVL1 and PDE4C mRNA. In short, RIP Lysis Buffer was employed to lyse the PTC cell lines and cell lysates were acquired by centrifugation. Subsequently, the cell lysates were incubated with Protein A/G magnetic beads coated with the ELAVL1 antibody (11910-1-AP, Proteintech, Wuhan, China) or rabbit IgG antibody (30000-0-AP, Proteintech), at 4°C overnight. Following the incubation, total RNA was extracted, and the level of PDE4C mRNA was quantitatively measured via quantitative real-time PCR (qRT-PCR).

mRNA stability assay

PTC cell lines were incubated with 5 μg/mL of actinomycin D (HY-17559, Medchem Express) to assess PDE4C mRNA stability. Cells were seeded in 6-well plates and treated with sh-ELAVL1-1/2. Next, cells were stimulated by actinomycin D for 0, 3 and 6 h, and the remaining PDE4C mRNA was measured by qRT-PCR analysis.

qRT-PCR analysis

Total RNA from PTC cell lines was isolated by TRIzol reagent (15596026CN, Invitrogen) referring to the manufacturer's manual. First Strand cDNA Synthesis Kit (P118-100, GeneBetter, Beijing, China) was conducted for reverse transcription. Next, qRT-PCR was conducted by SYBR Green qPCR Mix (P611-500, GeneBetter) on a Real-Time PCR System (ABI7300, Applied Biosystems). The amplification conditions were as follows: initial denaturation at 94°C for 2 min, followed by 40 cycles of denaturation at 94°C for 10 sec and annealing/extension at 60°C for 30 sec. The relative mRNA expression were described via the $2^{-\Delta\Delta Ct}$ method. Primers are listed in **Table 1**.

Western blot assay

RIPA Lysis Buffer (P0013, Beyotime, Shanghai, China) was employed to extract the total protein from PTC cell lines. Subsequently, the BCA Protein Quantification Kit (23225, Thermo Scientific) was applied for quantifying protein concentration. Equal samples (30 μg) underwent electrophoresis in SDS-PAGE and trans-

ferred to PVDF membranes (IPVH00010, Millipore). Then the membranes were blocked and incubated overnight at 4°C with primary antibodies, including anti-ELAVL1 (11910-1-AP, Proteintech, 1:2000), PDE4C (21754-1-AP, Proteintech, 1:500), and GAPDH (60004-1-Ig, Proteintech, 1:50000). Finally, the membranes were stimulated by secondary antibody (S0001 or S0002, Affinity Biosciences, 1:5000) and visualization was achieved using ECL reagent (32209, Thermo Scientific).

Animal experiments

Four-week-old female BALB/c nude mice (Shanghai SLAC Laboratory Animal Co., Ltd., China) were randomly allocated into three groups (n = 6 per group): sh-ELAVL1-2 group, sh-PDE4C-2 group, and sh-NC group. BCPAP cells (1×10^6 cells) treated with sh-ELAVL1-2 or sh-PDE4C-2 lentiviral vectors (HanBio, Shanghai, China) were injected into the footpads or subcutaneously into the mice, respectively, to observe *in vivo* LNM and tumor formation in PTC. The tumor sizes of the mice were gauged and recorded every 7 days, and the tumor volume was calculated following the formula volume (mm^3) = 0.5 × (length × $width^2$). Following the 6-week experimental period, all mice were subjected to terminal anesthesia with an overdose of sodium pentobarbital (100 mg/kg, i.p.) and subsequently euthanized via cervical dislocation to ensure humane endpoints. Samples of the primary tumor tissues and inguinal lymph nodes were collected for following experiments. Animal study was approved by the Institutional Animal Care and Use Committee of Zhejiang Provincial Laboratory Animal Center (Approval No.: ZJCLA-IACUC-20011158).

Immunohistochemistry (IHC)

Tissues from human PTC and subcutaneous tumor tissues of nude mice were subjected to fixation in 4% paraformaldehyde. After dehydration, the tissues were embedded in paraffin and cut into a thickness of 5 μm. Following deparaffinization and rehydration, the sections were treated with bovine serum albumin for 30 min and incubated with primary antibodies, including PDE4C (DF3872, Affinity Biosciences, 1:50), ELAVL1 (DF6496, Affinity Biosciences, 1:50), and Ki-67 (AF0198, Affinity Biosciences, 1:50), at 4°C throughout the night. Next, the sections were exposed to the corresponding secondary antibodies, stained with diaminobenzidine (DAB; AR1027, Boster, Wuhan, China), and counterstained with hematoxylin staining solution (G1080, Solarbio, Beijing, China). Images were acquired on a microscope (Zeiss, Germany).

Hematoxylin-eosin (HE) staining

The HE Stain Kit (G1120, Solarbio) was used to assess the number of metastatic tumors in the lymph nodes. Briefly, sections were deparaffinized with xylene, followed by a rehydration process through a series of graded ethanol solutions. Subsequently, the tissues were rinsed with distilled water, stained with hematoxylin solution, and counterstained with eosin in accordance with ptotocal. After staining, the sections were dehydrated through an ascending ethanol series, and mounted with neutral gum (G8590, Solarbio). Finally, metastatic tumor foci in the lymph nodes were examined under a light microscope (Zeiss, Germany).

Statistical analysis

The experimental data are presented as mean ± standard deviation. Statistical comparisons were performed using Student's t-test or one-way ANOVA followed by Tukey's post-hoc test. For comparisons across multiple time points, ANOVA with Tukey's post-hoc test was conducted using data from each group at the final time point. Every experiment was replicated a minimum of three times. GraphPad Prism 10.2.3 software (La Jolla, CA, USA) was used for statistical analysis. Statistical significance was set at $P < 0.05$.

Results

PDE4C is highly expressed in PTC

First, we assessed the expression level of PDE4C in thyroid cancer. UALCAN database analysis displayed that PDE4C expression was remarkably elevated in thyroid cancer tissues compared to adjacent normal tissues (**Figure 1A**). Furthermore, PDE4C was highly expressed in thyroid cancer tissues relative to normal tissues, as confirmed by GEPIA2 database analysis (**Figure 1B**). Results in **Figure 1C** further demonstrated that PDE4C was notably upregu-

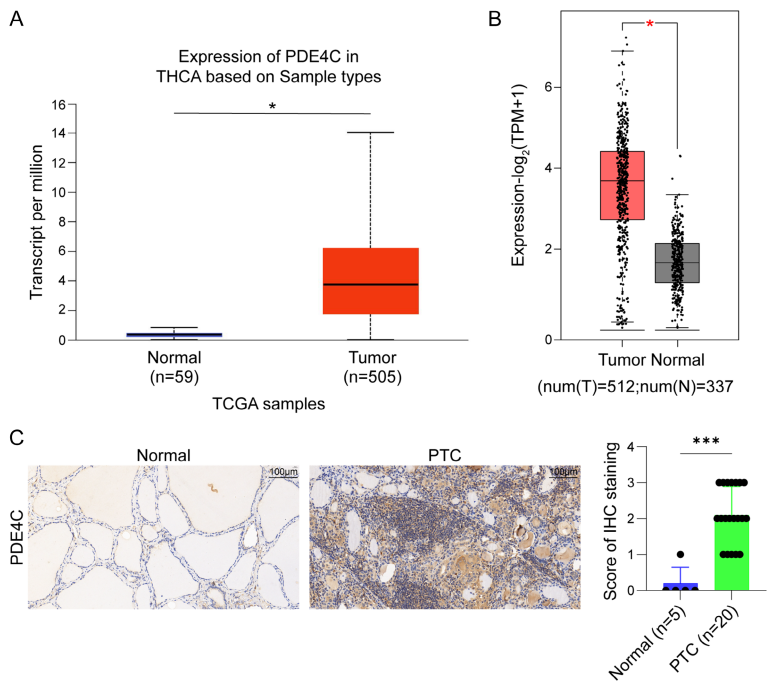

Figure 1. Phosphodiesterase 4C (PDE4C) is highly expressed in papillary thyroid carcinoma (PTC). A. PDE4C expression in thyroid carcinoma was statistically significant in UALCAN database. B. GEPIA2 database analysis of PDE4C expression in thyroid carcinoma. C. PDE4C expression in adjacent tumor tissues and PTC tissues were evaluated by immunohistochemistry (IHC) staining; scale bar: 100 μm, magnification: 40×. *$P < 0.05$, ***$P < 0.001$.

lated in PTC tissues compared with adjacent normal tissues. These data collectively indicate that PDE4C may be a potential regulator of PTC biological behaviour.

PDE4C knockdown inhibits the malignant phenotype of PTC cells

Given the high expression of PDE4C in PTC, this study employed sh-PDE4C-1 and sh-PDE4C-2 transfection techniques to establish PDE4C knockdown models in BCPAP and TPC-1 cell lines. Western blot and qRT-PCR analyses confirmed significant reductions in both PDE4C mRNA and protein levels (**Figure 2A**, **2B**). Functional assays revealed that PDE4C knockdown markedly inhibited cellular proliferation activity as assessed by CCK-8 assays, compared with the sh-NC group (**Figure 2C**). Transwell assays further demonstrated that PDE4C interference effectively suppressed cell migration and invasion capabilities (**Figure 2D**, **2E**). Collectively, these findings indicate that PDE4C promotes the proliferation, migration, and invasion of thyroid carcinoma cells *in vitro*.

ELAVL1 interacts with PDE4C and enhances its mRNA stability

To elucidate the upstream regulatory mechanism of PDE4C in thyroid carcinoma, we first utilised the ENCORI database to predict potential binding between the RNA-binding protein ELAVL1 and PDE4C mRNA (**Figure 3A**). RNA precipitation experiments confirmed that ELAVL1 directly binds to PDE4C mRNA (**Figure 3B**). Further RIP revealed significantly enhanced enrichment of PDE4C mRNA in the ELAVL1 antibody group compared to the IgG control group (**Figure 3C**). qRT-PCR and Western blot analyses demonstrated that PDE4C expression was markedly reduced at both mRNA and protein levels following ELAVL1 knockdown (**Figure 3D**, **3E**). We also observed that ELAVL1 depletion markedly decreased PDE4C mRNA stability (**Figure 3F**), suggesting that ELAVL1 binds to PDE4C mRNA and enhances its stability.

ELAVL1 is highly expressed in PTC

Next, we examined the expression level of ELAVL1 in PTC. UALCAN analysis revealed significantly elevated ELAVL1 levels in thyroid cancer tissues as opposed to adjacent normal tissues (**Figure 4A**). We also performed GEPIA2 analysis to compare the ELAVL1 expression in thyroid cancer tissues and normal tissues. As presented in **Figure 4B**, ELAVL1 was upregulated in thyroid cancer tissues relative to normal tissues. Further validation via IHC confirmed stronger ELAVL1 staining in PTC tissues relative to adjacent normal controls (**Figure 4C**). These results revealed that ELAVL1 is overexpressed in PTC, suggesting its potential oncogenic role.

ELAVL1/PDE4C axis regulates the proliferation, migration, and invasion of PTC cells

Western blot and qRT-PCR suggested that PDE4C overexpression remarkably upregulated

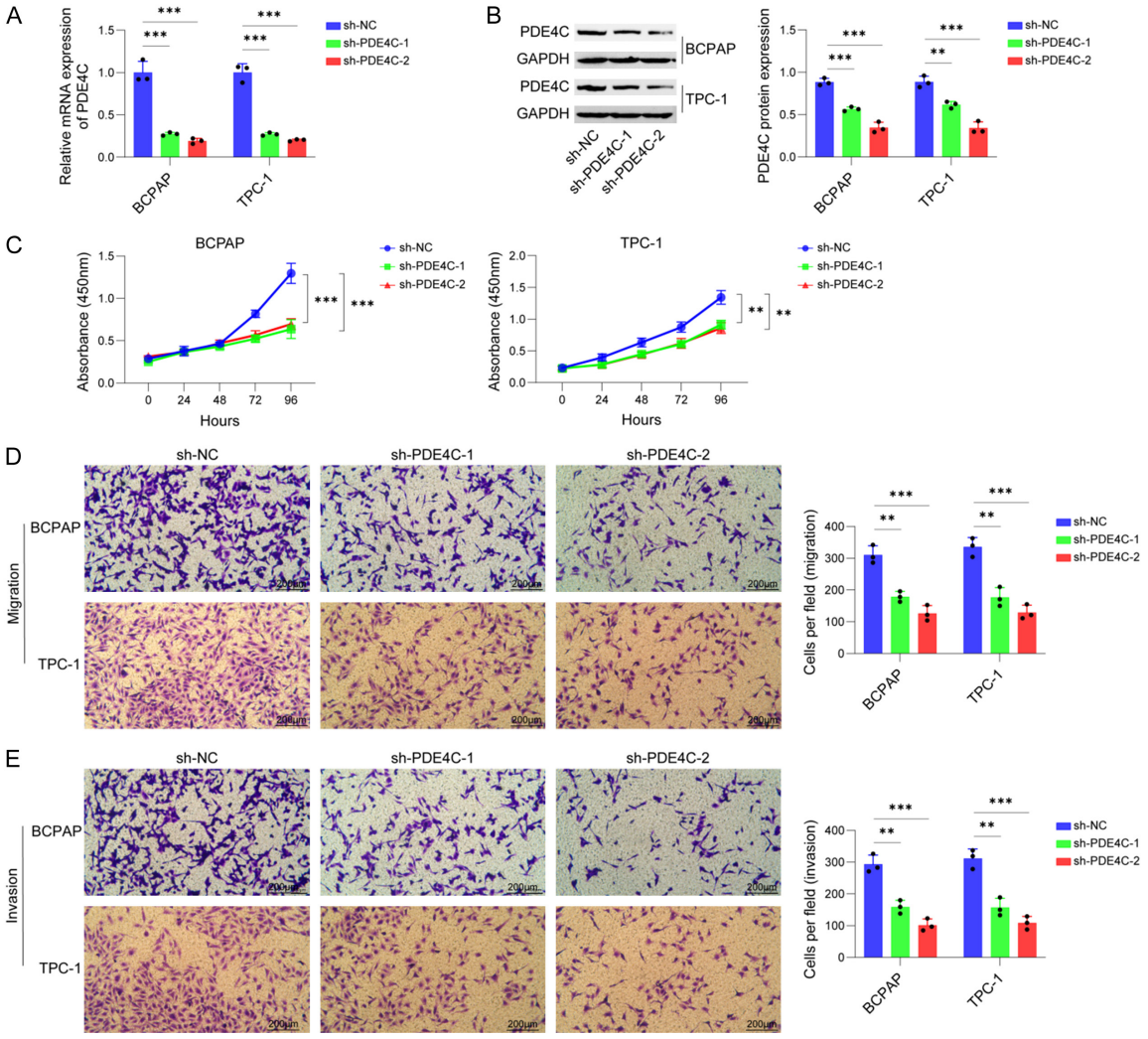

Figure 2. Effects of PDE4C on PTC cell proliferation, migration, and invasion. A, B. The expression of PDE4C was verified by quantitative real-time PCR (qRT-PCR) and Western blot. C. Proliferation of PTC cells was determined using cell counting kit-8 (CCK-8) assay. D. Representative images and histogram analysis of migrated cells after PDE4C knockdown; scale bar: 200 μm, magnification: 10×. E. The number of invaded cells was determined using Transwell assay; scale bar: 200 μm, magnification: 10×. $^{**}P < 0.01$, $^{***}P < 0.001$.

both PDE4C mRNA and protein levels (**Figure 5A**, **5B**). Next, BCPAP and TPC-1 cells were co-transfected with sh-ELAVL1 and/or oe-PDE4C to investigate whether PDE4C could abolish the effects of ELAVL1 knockdown on malignant phenotypes of PTC cells. Results in **Figure 5C** revealed that ELAVL1 knockdown notably attenuated PTC cell proliferation, whereas PDE4C overexpression partially restored proliferative capacity. Besides, ELAVL1 knockdown markedly inhibited PTC cell migration and invasion, as revealed by Transwell assays. However, these effects were partially counteracted by PDE4C overexpression (**Figure 5D**, **5E**). These observations suggested that ELAVL1 enhances PTC cell proliferation, migration, and invasion by upregulating PDE4C.

Silencing of PDE4C or ELAVL1 inhibits PTC growth and LNM

To illustrate the function of ELAVL1/PDE4C axis in lymphatic metastasis of PTC, BCPAP cells were injected into the tissues surrounding the footpads of mice to construct LNM models (**Figure 6A**). The knockdown of ELAVL1 or PDE4C obviously decreased the number of tumor cells in lymph nodes compared with the sh-NC treated mice (**Figure 6B**). Moreover, the functional role of ELAVL1/PDE4C in PTC tumor

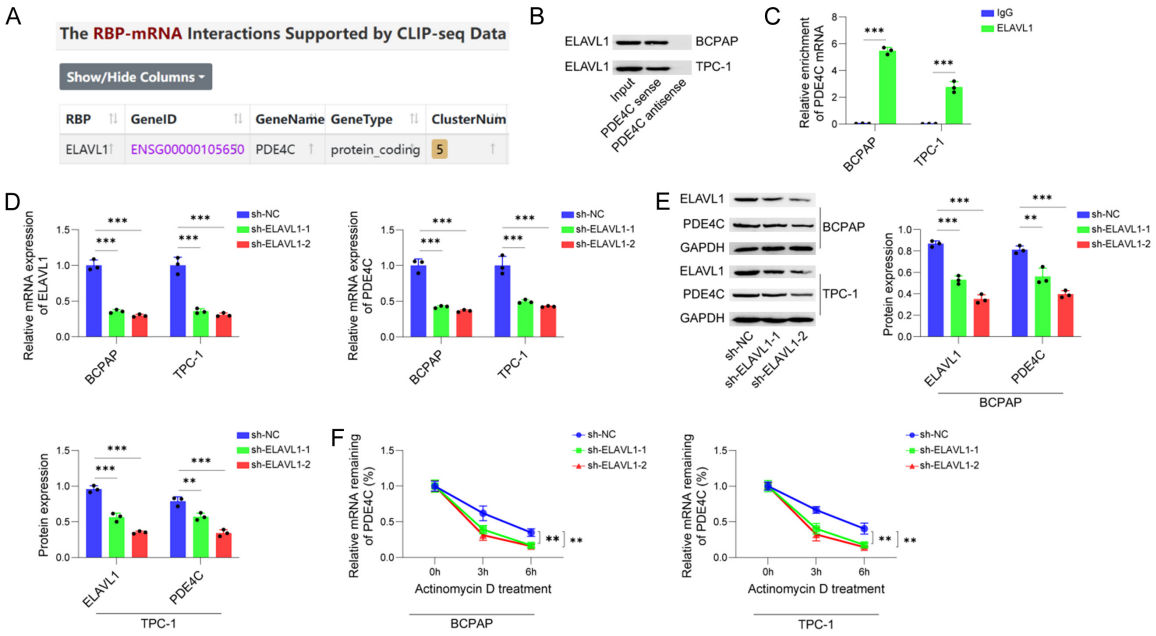

Figure 3. ELAVL1 stabilizes PDE4C mRNA through direct interaction. A. ENCORI database predicted that ELAVL1 binds to PDE4C. B. RNA pull down verified that ELAVL1 binds to PDE4C mRNA. C. ELAVL1 and PDE4C mRNA interaction was confirmed via RNA immunoprecipitation (RIP) assay. D. The mRNA levels of ELAVL1 and PDE4C were determined using qRT-PCR. E. ELAVL1 and PDE4C protein levels were assessed by Western blot. F. PDE4C mRNA stability was evaluated via qRT-PCR. $^{**}P < 0.01$, $^{***}P < 0.001$.

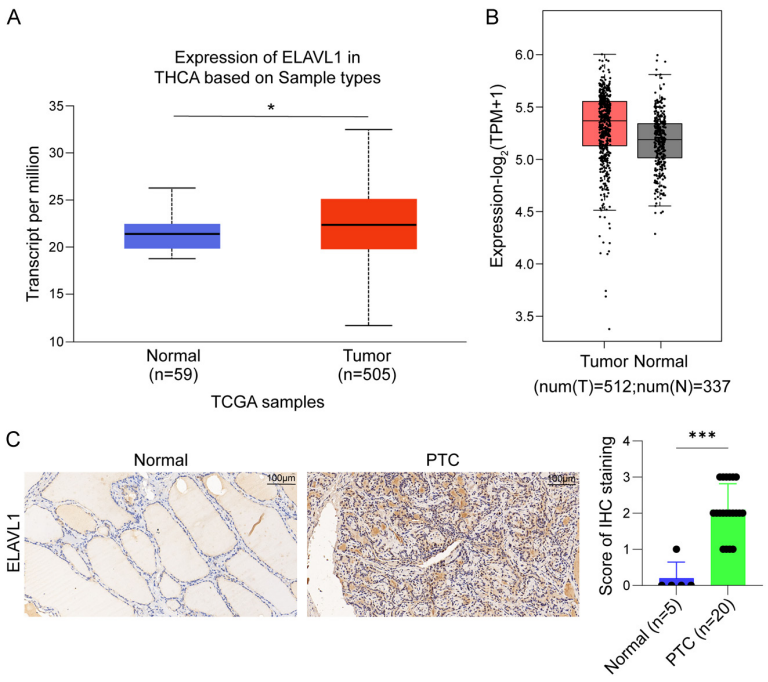

Figure 4. ELAVL1 is overexpressed in PTC. A. UALCAN analysis of ELAVL1 expression in thyroid carcinoma. B. GEPIA2 database analysis of ELAVL1 expression in thyroid carcinoma. C. Expression of ELAVL1 in adjacent tumor tissues and PTC tissues were determined by IHC staining; scale bar: 100 μm, magnification: 40×. $^{*}P < 0.05$, $^{***}P < 0.001$.

growth was evaluated, BCPAP cells treated with sh-NC, sh-ELAVL or sh-PDE4C were injected subcutaneously into the mice (**Figure 6A**). Results in **Figure 6C-E** revealed that knockdown of ELAVL1 or PDE4C remarkably inhibited PTC tumor growth, reduced tumor volume, and decreased tumor weight. Immunohistochemical analysis further confirmed these findings, showing a significant decrease in Ki-67 expression after knockdown of ELAVL1 or PDE4C (**Figure 6F**). These data demonstrated that knockdown of ELAVL1 or PDE4C inhibits PTC growth and LNM.

Discussion

PTC represents the most common endocrine malignancy, with a persistent global increase in incidence in re-

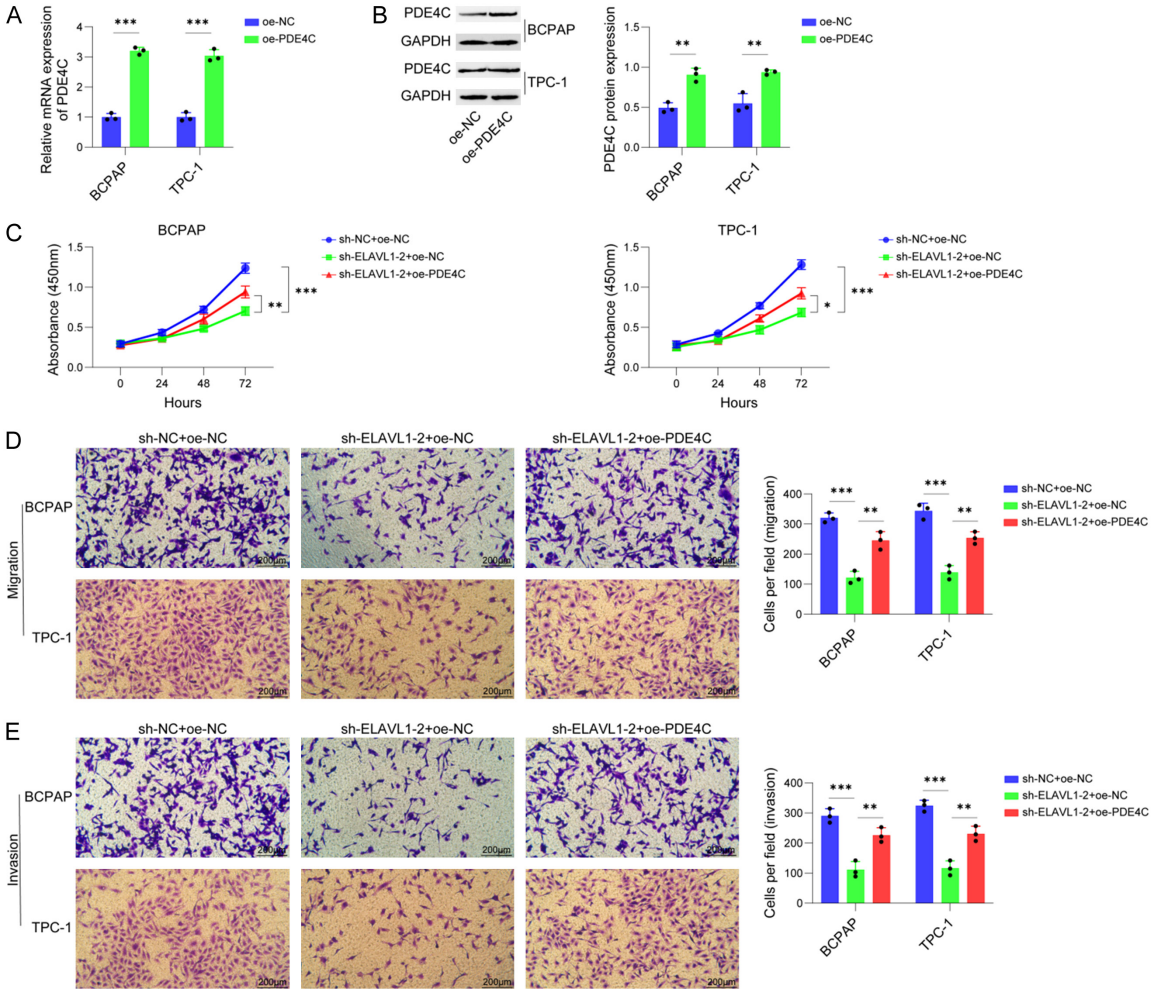

Figure 5. ELAVL1 silence suppresses PTC cell proliferation, migration, and invasion by regulating PDE4C. A. qRT-PCR analysis of the PDE4C expression in oe-PDE4C/oe-NC transfected PTC cells. B. Western blot for PDE4C levels. C. CCK-8 revealed proliferation after transfection with oe-PDE4C and/or sh-ELAVL1 in PTC cells. D. Representative images and histogram analysis of migrated cells; scale bar: 200 μm, magnification: 10×. E. The number of invaded cells was determined using Transwell assay; scale bar: 200 μm, magnification: 10×. *$P < 0.05$, **$P < 0.01$, ***$P < 0.001$.

cent years [17]. Although most patients with PTC exhibit favourable outcomes following standardised treatment, the occurrence of LNM significantly impacts survival outcomes and recurrence risk [18]. Thus, elucidating the molecular pathogenesis of PTC is essential for developing effective therapeutic strategies. This study focuses on the functional role and regulatory mechanisms of PDE4C in PTC progression. We discovered that PDE4C expression is markedly elevated in PTC tissues and is positively regulated by the RNA-binding protein ELAVL1 through mRNA stabilisation. ELAVL1 enhances PTC cell proliferation, migration, invasion, tumor growth, and LNM by stabilizing PDE4C mRNA. In summary, this study suggests that PDE4C may represent a key regulatory molecule involved in the initiation and progression of PTC.

PDEs, as a key family of enzymes hydrolysing intracellular second messengers cAMP and cGMP, play a crucial regulatory role in maintaining the dynamic equilibrium of cyclic nucleotide signalling pathways [19]. Recent studies have revealed that PDEs may contribute to tumor progression and metastasis by modulating the tumor microenvironment, cellular metabolism, and intracellular signaling. For example, PDE4A enhances tumor cell activities by promoting proliferation, migration, invasion, and stemness characteristics of esophageal squamous

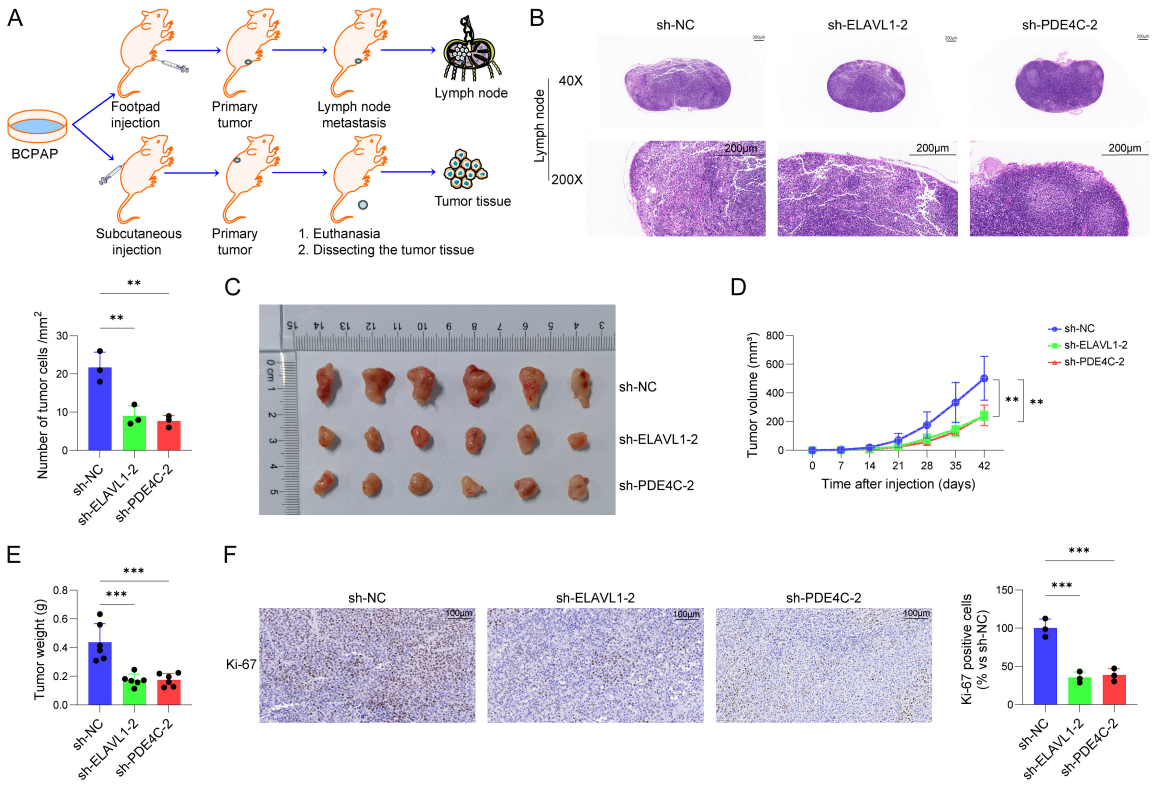

Figure 6. PDE4C or ELAVL1 enhances tumor growth and lymphatic metastatic potential of PTC *in vivo*. A. Schematic representation of *in vivo* lymphatic metastasis (upper panel) and subcutaneous injection (lower panel) models. B. Hematoxylin-eosin (HE) staining was performed to evaluate lymph node tumors; scale bar: 200 μm, magnification: 40× and 200×. C. Representative tumors formed by BCPAP cells in each group. D. The effect of ELAVL1 or PDE4C silence on the tumor volumes in each groups. E. The effect of ELAVL1 or PDE4C silence on the tumor weights in each groups. F. The representative images of Ki-67 staining; scale bar: 100 μm, magnification: 40×. $^{**}P < 0.01$, $^{***}P < 0.001$.

cell carcinoma cells, while also suppressing apoptosis [20]; PDE4B facilitats cell proliferation, migration/invasion, and epithelial-to-mesenchymal transition in urinary bladder cancer [21]; Pancreatic cancer is characterized by an upregulation of PDE4D expression, and elevated levels of PDE4D are linked to poor overall survival of patients [22]. As an important member of the PDE family, PDE4C was evidenced to be involved in the progression of many cancers. PDE4C was confirmed to be overexpressed in thyroid carcinoma [23], osteosarcoma [11], and adenomyosis [24]. Furthermore, elevated PDE4C expression has been identified as a candidate diagnostic biomarker and is linked to poor survival in diseases. For instance, Su et al. revealed that knockdown of PDE4C in PTC cells induces the inhibitory roles in proliferation, migration, and invasion, highlighting its possibility of being a treatment target [10]. Our study revealed that PDE4C was notably overexpressed in PTC tissues, suggesting its potential as a biomarker. Moreover, knockdown of PDE4C markedly inhibited the proliferation, migration, and invasion of PTC cells, suggesting its role in promoting tumor metastasis [11, 25]. Notably, *in vivo* experiments confirmed that silencing PDE4C effectively suppresses tumor growth and LNM, thereby corroborating its pivotal function as a metastasis driver at the systemic level.

ELAVL1 is a crucial RNA-binding protein that has been demonstrated to participate in the initiation and progression of multiple tumors [26]. Previous studies indicate that ELAVL1 can specifically bind target RNAs, thereby regulating key cellular processes such as proliferation, differentiation, and apoptosis [27, 28]. Additionally, ELAVL1 is highly expressed in PTC and exerts oncogenic effects by stabilising target transcripts [16]. Knockdown of ELAVL1 has

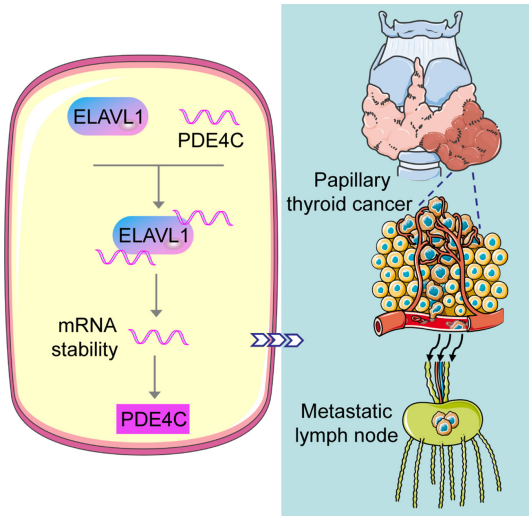

Figure 7. The mechanism of PDE4C regulatory roles in lymph node metastasis of PTC. Schematic illustration revealing that ELAVL1 enhances the PDE4C mRNA stability by interacting with PDE4C. This interaction promotes PTC growth and lymph node metastasis.

been shown to enhance PTC cell viability and decrease migratory capacity [29]. This study predicts and identifies PDE4C as a novel binding target for ELAVL1. Subsequent experiments confirmed that ELAVL1 directly binds to PDE4C mRNA, thereby enhancing its stability and upregulating its expression. To our knowledge, this is the first report establishing a functional relationship between PDE4C and ELAVL1, highlighting their roles in PTC pathogenesis. We further discovered that silencing ELAVL1 significantly suppressed the malignant phenotype of tumor cells and *in vivo* tumor progression, whereas PDE4C overexpression partially reversed this inhibitory effect, consistent with prior studies [16]. Notably, the ELAVL1/PDE4C regulatory axis was found to regulate the malignant cellular behaviors of PTC cells and modulate tumor growth and LNM. These results suggested that the axis may promote PTC invasiveness by augmenting tumor cell proliferation and metastatic potential.

Collectively, we identified the ELAVL1/PDE4C axis as a critical promoter of PTC progression and lymph node metastasis (**Figure 7**), confirming that ELAVL1 promotes tumor growth and invasion by stabilising PDE4C mRNA. PDE4C may serve as a predictive biomarker and therapeutic target for PTC. However, our study has several limitations. Firstly, the downstream signaling mechanism of PDE4C in PTC remain incompletely elucidated, and its interaction with the cAMP/cGMP-dependent pathway needs to be further investigated. Secondly, although *in vivo* experiments consistently demonstrate that knocking down ELAVL1 or PDE4C alone suppresses tumor growth, the lack of rescue experiments limits functional validation. Further studies are needed to confirm the role of this axis in more physiologically relevant models.

Acknowledgements

This work was supported by the Science and Technology Plan Project of Taizhou (grant number: 23ywa49).

Disclosure of conflict of interest

None.

Address correspondence to: Tingting Cui, Department of Ultrasound, Taizhou Traditional Chinese Medicine Hospital, No. 278 Zhongshan West Road, Jiaojiang 318000, Zhejiang, China. Tel: +86-576-88825602; Fax: +86-576-88825602; E-mail: cuitingting0708@163.com

References

[1] Boucai L, Zafereo M and Cabanillas ME. Thyroid cancer: a review. JAMA 2024; 331: 425-435.
[2] Lam AK. Papillary thyroid carcinoma: current position in epidemiology, genomics, and classification. Methods Mol Biol 2022; 2534: 1-15.
[3] Zhang J, Chen C, Yang Y and Zhang B. Surgical resection following therapy with anlotinib in locally advanced papillary thyroid carcinoma: a case description. Quant Imaging Med Surg 2023; 13: 5456-5462.
[4] Chan WWL and Kwong DLW. Radioactive Iodine for papillary thyroid carcinoma. Methods Mol Biol 2022; 2534: 225-241.
[5] Zhou J, Li DX, Gao H and Su XL. Relationship between subgroups of central and lateral lymph node metastasis in clinically node-negative papillary thyroid carcinoma. World J Clin Cases 2022; 10: 3709-3719.
[6] Wang K, Li H, Zhao J, Yao J, Lu Y, Dong J, Bai J and Liao L. Potential diagnostic of lymph node metastasis and prognostic values of TM4SFs in papillary thyroid carcinoma patients. Front Cell Dev Biol 2022; 10: 1001954.
[7] Moon S, Song YS, Jung KY, Lee EK and Park YJ. Lower thyroid cancer mortality in patients detected by screening: a meta-analysis. Endocrinol Metab (Seoul) 2023; 38: 93-103.

[8] Mayora Justel C, Valladares T, Gargiulo L, González-Pardo V, De Sousa M, Esandi MDC, Davio C, Lüthy I and Bruzzone A. Inhibition of phosphodiesterase 4 and 7 regulates breast cancer cell proliferation. Biochim Biophys Acta Gen Subj 2025; 1869: 130850.
[9] Wright TA, Gemmell AO, Tejeda GS, Blair CM and Baillie GS. Cancer: phosphodiesterase type 4C (PDE4C), the forgotten subfamily as a therapeutic target. Int J Biochem Cell Biol 2023; 162: 106453.
[10] Su Y, Xu B, Gao C, Pei W, Ma M, Zhang W, Hu T, Zhang F and Zhang S. HNF4α-mediated LINC02560 promotes papillary thyroid carcinoma progression by targeting the miR-505-5p/PDE4C axis. Biomolecules 2025; 15: 630.
[11] Pan F, Pan R, Hu R, Zhang H, Lei S, Zhang L, Zhou C, Zeng Z, Tian X and Xie Q. Analysis of the effects of M2 macrophage-derived PDE4C on the prognosis, metastasis and immunotherapy benefit of osteosarcoma. J Cell Mol Med 2024; 28: e18395.
[12] Zhao X, Su F, Guo Q, Tao X, Wang H, Wang H, Li Q and Zhang W. Preeclampsia-associated lncRNA FEZF1-AS1 regulates cell proliferation and apoptosis in placental trophoblast cells through the ELAVL1/NOC2L axis. Cell Div 2023; 18: 17.
[13] Jiang T, Bo S, You Y, Wang Y, Hou L, Tian S, Bai B, Cheng Y and Gao Y. ELAVL1 facilitates gastric cancer progression and metastasis through TL1A mRNA stabilization. Exp Cell Res 2025; 446: 114491.
[14] Cai Z, Xu H, Bai G, Hu H, Wang D, Li H and Wang Z. ELAVL1 promotes prostate cancer progression by interacting with other m6A regulators. Front Oncol 2022; 12: 939784.
[15] Wang X, Liu D, Hua K and Fang L. LncRNA HOST2 promotes NSUN2-mediated breast cancer progression via interaction with ELAVL1. Cell Signal 2024; 117: 111112.
[16] Liu Y, Xin Y, Shang X, Tian Z and Xue G. CircSEMA6A upregulates PRRG4 by targeting MiR-520h and recruiting ELAVL1 to affect cell invasion and migration in papillary thyroid carcinoma. Arch Endocrinol Metab 2024; 68: e210541.
[17] Yan K, Liu QZ, Huang RR, Jiang YH, Bian ZH, Li SJ, Li L, Shen F, Tsuneyama K, Zhang QL, Lian ZX, Guan H and Xu B. Spatial transcriptomics reveals prognosis-associated cellular heterogeneity in the papillary thyroid carcinoma microenvironment. Clin Transl Med 2024; 14: e1594.
[18] Liu W, Zheng J, Han L, Qu W, Wu Q, Yuan Z, Jia G, Wang X, Ye L, Zhang J, Zhang S, Cao X, Liu Y and Ai Z. Clinical performance of a machine learning-based model for detecting lymph node metastasis in papillary thyroid carcinoma: a multicenter study. Int J Surg 2025; 111: 4062-4067.
[19] Kamel R, Leroy J, Vandecasteele G and Fischmeister R. Cyclic nucleotide phosphodiesterases as therapeutic targets in cardiac hypertrophy and heart failure. Nat Rev Cardiol 2023; 20: 90-108.
[20] Xu J, Ma J, Guan B, Li J, Wang Y and Hu S. LncRNA HCP5 promotes malignant cell behaviors in esophageal squamous cell carcinoma via the PI3K/AKT/mTOR signaling. Cell Cycle 2021; 20: 1374-1388.
[21] Huang Z, Liu J, Yang J, Yan Y, Yang C, He X, Huang R, Tan M, Wu D, Yan J and Shen B. PDE4B induces epithelial-to-mesenchymal transition in bladder cancer cells and is transcriptionally suppressed by CBX7. Front Cell Dev Biol 2021; 9: 783050.
[22] Jeong MH, Urquhart G, Lewis C, Chi Z and Jewell JL. Inhibition of phosphodiesterase 4D suppresses mTORC1 signaling and pancreatic cancer growth. JCI Insight 2023; 8: e158098.
[23] Wang Y, Zhang Y, Li Y and Huang J. Elevated PDE4C level serves as a candidate diagnostic biomarker and correlates with poor survival in thyroid carcinoma. Sci Rep 2024; 14: 6813.
[24] Wu Z, Ren H and Guo F. Pan-cancer analysis of cyclic nucleotide phosphodiesterases (PDEs) expression, variation, and prognostic significance. ACS Omega 2025; 10: 61247-61255.
[25] Hsien Lai S, Zervoudakis G, Chou J, Gurney ME and Quesnelle KM. PDE4 subtypes in cancer. Oncogene 2020; 39: 3791-3802.
[26] Zhang X, Wang J, Liang X, Jiang D, Sun Y, Hu C, Hu F, He Y, Sun Y, Zhang J, Ding J, Cai S, Wang Y, Yang S and Yang K. BAP31-ELAVL1-SPINK6 axis induces loss of cell polarity and promotes metastasis in hepatocellular carcinoma. Int J Biol Sci 2025; 21: 1632-1648.
[27] Cao S, Li C, Li L, Zhou G, Jiang Y and Feng J. Circular RNA hsa_circ_0000848 regulates cardiomyocyte proliferation and apoptosis under hypoxia via recruiting ELAVL1 and stabilizing SMAD7 mRNA. Anatol J Cardiol 2022; 26: 189-197.
[28] Ye W, Liu Z, Liu Y, Xiao H, Tan Q, Yan A and Zhu G. ELAVL1 promotes ferroptosis via the TRIM21/HOXD8 axis to inhibit osteogenic differentiation in congenital pseudoarticular tibia-derived mesenchymal stem cells. J Cell Commun Signal 2025; 19: e70016.
[29] Wu D, Wang B, Shang J, Song J and Zhang H. miR-31 reduces cell growth of papillary thyroid carcinoma by RNA-binding protein HuR. Clin Lab 2015; 61: 1625-1634.